ISSN 1512-1461

UDC: 538.9 Condensed matter Physics, Solid state Physics, Theoretical Condensed matter Physics

FCC STRUCTURED FERROMAGNETIC FILMS WITH THREE SPIN LAYERS AS DESCRIBED BY FOURTH ORDER PERTURBED HEISENBERG HAMILTONIAN

N.U.S. Yapa[1] and Sara N. Samarasekara[2]
[1]Department of Physics, Open University of Sri Lanka, Kandy, Sri Lanka
[2]Cullen College of engineering, University of Houston, Houston, TX77004, USA

Abstract:
Fourth order perturbed Heisenberg Hamiltonian was employed to determine the magnetic easy and hard directions of fcc structured ferromagnetic thin films with three spin layers. Only the spin exchange interaction, long range dipole interaction and second order magnetic anisotropy terms were taken into account. 3D graphs of total magnetic energy versus angle and spin exchange interaction were plotted for different values of second order magnetic anisotropy constants in three spin layers. In 3D plots, the peaks along the axis of angle are closely packed. However, some periodic variation of energy was observed along the axis of spin exchange interaction in 3D plots. The order of energy varies from 10^{14} to 10^{16} in these 3D plots. In addition, the graphs of energy versus angle were plotted in order to determine the magnetic easy and hard directions.

Keywords: *Heisenberg Hamiltonian, fourth order perturbation, fcc structure, ferromagnetic.*

1. Introduction:

Ferromagnetic thin films are prime candidates in transformers, electromagnets, magnetic tape recording, sensors, actuators and hard drives. Landau Lifshitz Gilbert equation has been employed to study the surface acoustic wave driven ferromagnetic resonance [1]. The time and frequency domain method has been used to investigate precessional magnetization behavior and damping in ferromagnetic thin films [2]. EuTe films with surface elastic stresses have been theoretically studied using Heisenberg Hamiltonian [3]. De Vries theory was employed to explain the magnetostriction of dc magnetron sputtered FeTaN thin films [4]. Magnetic layers of Ni on Cu have been theoretically investigated using the Korringa-Kohn-Rostoker Green's function method [5]. Electric and magnetic properties of multiferroic thin films have been theoretically described using modified Heisenberg model and transverse Ising model coupled with Green's function technique [6].

The interfacial coupling dependence of the magnetic ordering in ferro-antiferromagntic bilayers has been studied using the Heisenberg Hamiltonian [7]. Heisenberg Hamiltonian incorporated with spin exchange interaction, magnetic dipole interaction, applied magnetic field, second and fourth order magnetic anisotropy terms has been solved for ferromagnetic thin films [8, 9, 10]. The domain structure and Magnetization reversal in thin magnetic films was described using computer simulations [11]. Heisenberg Hamiltonian has been employed to theoretically describe in-plane dipole coupling anisotropy of a square ferromagnetic Heisenberg monolayer [12].

Previously magnetic thin films have been fabricated using sputtering and pulse laser deposition techniques by us [13-15]. According to our experimental studies, some magnetic energy parameters were found to be important in the control of magnetic easy axis orientation. Ferrite films have been explained using second order perturbed Heisenberg Hamiltonian by us [16, 17]. In addition, Heisenberg Hamiltonian was employed to describe the variation of magnetic easy axis orientation

ISSN 1512-1461

of experimentally deposited magnetic thin films with temperature [18]. Second and third order perturbed Heisenberg Hamiltonian was applied to explain the ferromagnetic films by us [19-22]. Unperturbed Heisenberg Hamiltonian was applied to describe ferrite thin films [23]. Magnetic properties of ferrite films have been elucidated using and third order perturbed Heisenberg Hamiltonian by us [24]. Magnetostatic energy of domains and domain walls has been theoretically investigated as a function of film thickness [25]. Magnetic thin films with thicknesses ranging from 2 to 4 layers have been modeled using anisotropic classical Heisenberg spins under the influence of mechanical uniaxial stresses [26]. Monte carlo simulation has been employed to study magnetic properties of very thin films with bcc lattice [27]. The properties of thin films made of stacked triangular layers of atoms bearing Heisenberg spins with an Ising like interaction anisotropy have been investigated using extensive Monte Carlo simulations and analytical Green's function [28]. Landau Lifshitz theory has been utilized to describe the initial complex permeability frequency spectra of thin soft ferromagnetic films with in-plane anisotropy [29].

2. Model:

Heisenberg Hamiltonian of ferromagnetic thin films with spin exchange interaction, long range dipole interaction and second order magnetic anisotropy can be expressed as [16. 17, 21-24].

$$H= -\frac{J}{2}\sum_{m,n}\vec{S}_m.\vec{S}_n+\frac{\omega}{2}\sum_{m\neq n}\left(\frac{\vec{S}_m.\vec{S}_n}{r_{mn}^3}-\frac{3(\vec{S}_m.\vec{r}_{mn})(\vec{r}_{mn}.\vec{S}_n)}{r_{mn}^5}\right)-\sum_m D_{\lambda_m}^{(2)}(S_m^z)^2 \qquad \textbf{(1)}$$

After taking the dot products of spin vectors in above equation, it can be deduced to the following form per unit spin with [16. 17, 21-24].

$$. E(\theta)= -\frac{1}{2}\sum_{m,n=1}^{N}\left[\left(JZ_{|m-n|}-\frac{\omega}{4}\Phi_{|m-n|}\right)\cos(\theta_m-\theta_n)-\frac{3\omega}{4}\Phi_{|m-n|}\cos(\theta_m+\theta_n)\right]$$
$$-\sum_{m=1}^{N}D_m^{(2)}\cos^2\theta_m \qquad \textbf{(2)}$$

Where *m* and *n* are the indices of two different spin layers, *N* is the number of layers measured in the direction perpendicular to the film plane, *J* is the magnetic spin-exchange interaction, $Z_{|m-n|}$ stands for the number of nearest spin neighbors, ω represents the strength of long-range dipole interaction, $\Phi_{|m-n|}$ are constants for partial summation of dipole interaction, For non-oriented films, above angles θ_m and θ_n measured with film normal can be expressed in forms of $\theta_m=\theta+\varepsilon_m$ and $\theta_n=\theta+\varepsilon_n$, and cosine and sine terms can be expanded up to the fourth-order of ε as following. Here ε indicates the perturbation of the angle. For a ferromagnetic thin film with three spin layers, *N* varies from 1 to 3.

$$E(\theta)=E_0+E(\varepsilon)+E(\varepsilon^2)+E(\varepsilon^3)+E(\varepsilon^4) \qquad \textbf{(3)}$$

$$E_0=-\frac{3}{2}\left(JZ_0-\frac{\omega\phi_0}{4}\right)-2\left(JZ_1-\frac{\omega\phi_1}{4}\right)+\frac{3\omega}{8}\left(3\phi_0+4\phi_1\right)\cos 2\theta$$
$$-\left(D_1^{(2)}+D_2^{(2)}+D_3^{(2)}\right)\cos^2\theta \qquad \textbf{(4)}$$

ISSN 1512-1461

$$E(\varepsilon) = -\frac{3\omega}{4}[\phi_0(\varepsilon_1 + \varepsilon_2 + \varepsilon_3) + \phi_1(\varepsilon_1 + 2\varepsilon_2 + \varepsilon_3)]\sin 2\theta + \sin 2\theta\left(D_1^{(2)}\varepsilon_1 + D_2^{(2)}\varepsilon_2 + D_3^{(2)}\varepsilon_3\right) \quad \textbf{(5)}$$

$$E(\varepsilon^2) = \left(JZ_1 - \frac{\omega\phi_1}{4}\right)\left(\frac{\varepsilon_1^2 + 2\varepsilon_2^2 + \varepsilon_3^2 - 2\varepsilon_1\varepsilon_2 - 2\varepsilon_2\varepsilon_3}{2}\right) - \frac{3\omega}{8}\cos 2\theta\left(2\phi_0(\varepsilon_1^2 + \varepsilon_2^2 + \varepsilon_3^2) + \phi_1\left(\varepsilon_1^2 + 2\varepsilon_2^2 + \varepsilon_3^2 + 2\varepsilon_1\varepsilon_2 + 2\varepsilon_2\varepsilon_3\right)\right) + \left(D_1^{(2)}\varepsilon_1^2 + D_2^{(2)}\varepsilon_2^2 + D_3^{(2)}\varepsilon_3^2\right)\cos 2\theta \quad \textbf{(6)}$$

$$E(\varepsilon^3) = \frac{\omega}{8}\begin{pmatrix} 4\phi_0(\varepsilon_1^3 + \varepsilon_2^3 + \varepsilon_3^3) + \phi_1(\varepsilon_1^3 + 3\varepsilon_1\varepsilon_2^2 + 3\varepsilon_1^2\varepsilon_2 + 2\varepsilon_2^3 \\ + 3\varepsilon_2\varepsilon_3^2 + 3\varepsilon_2^2\varepsilon_3 + \varepsilon_3^3) \end{pmatrix}\sin 2\theta - \frac{4\cos\theta\sin\theta}{3}\left(D_1^{(2)}\varepsilon_1^3 + D_2^{(2)}\varepsilon_2^3 + D_3^{(2)}\varepsilon_3^3\right) \quad \textbf{(7)}$$

$$E(\varepsilon^4) = \left(\frac{\omega}{4}\phi_1 - JZ_1\right)\begin{pmatrix} \varepsilon_1^4 + 2\varepsilon_2^4 + \varepsilon_3^4 + 6\varepsilon_1^2\varepsilon_2^2 \\ \frac{-4\varepsilon_1^3\varepsilon_2 - 4\varepsilon_1\varepsilon_2^3 + 6\varepsilon_2^2\varepsilon_3^2 - 4\varepsilon_2^3\varepsilon_3 - 4\varepsilon_2\varepsilon_3^3}{24} \\ \end{pmatrix} + \frac{\omega}{8}\cos 2\theta\{\left[2\phi_0\left(\varepsilon_1^4 + \varepsilon_2^4 + \varepsilon_3^4\right)\right] + \frac{\phi_1}{4}\begin{pmatrix} \varepsilon_1^4 + 2\varepsilon_2^4 + \varepsilon_3^4 + 6\varepsilon_1^2\varepsilon_2^2 + 4\varepsilon_1^3\varepsilon_2 + 4\varepsilon_1\varepsilon_2^3 \\ + 6\varepsilon_2^2\varepsilon_3^2 + 4\varepsilon_2^3\varepsilon_3 + 4\varepsilon_2\varepsilon_3^3 \end{pmatrix}\} - \frac{\cos 2\theta}{3}\left(D_1^{(2)}\varepsilon_1^4 + D_2^{(2)}\varepsilon_2^4 + D_3^{(2)}\varepsilon_3^4\right) \quad \textbf{(8)}$$

Where $D_1^{(2)}$, $D_2^{(2)}$ and $D_3^{(2)}$ represent the second-order anisotropy constants of bottom, middle and top spin layers, respectively.

By comparing the coefficients in equation $E(\varepsilon)=\vec{\alpha}.\vec{\varepsilon}$, α_1, α_2 and α_3 can be found.

$$\alpha_1 = -\frac{3\omega}{4}(\phi_0 + \phi_1)\sin 2\theta + D_1^{(2)}\sin 2\theta$$

$$\alpha_2 = -\frac{3\omega}{4}(\phi_0 + 2\phi_1)\sin 2\theta + D_2^{(2)}\sin 2\theta$$

$$\alpha_3 = -\frac{3\omega}{4}(\phi_0 + \phi_1)\sin 2\theta + D_3^{(2)}\sin 2\theta$$

Matrix elements of matrix C can be determined by

ISSN 1512-1461

$$E(\varepsilon^2) = \frac{1}{2}\vec{\varepsilon}.C.\vec{\varepsilon}$$

$$C_{11} = JZ_1 - \frac{\omega\phi_1}{4} - \frac{3\omega}{4}(2\phi_0 + \phi_1)\cos 2\theta + 2D_1^{(2)}\cos 2\theta$$

$$C_{12} = C_{21} = C_{23} = C_{32} = -JZ_1 + \frac{\omega\phi_1}{4} - \frac{3\omega}{4}\phi_1\cos 2\theta$$

$$C_{13} = C_{31} = 0$$

$$C_{22} = 2(JZ_1 - \frac{\omega\phi_1}{4}) - \frac{3\omega}{2}(\phi_0 + \phi_1)\cos 2\theta + 2D_2^{(2)}\cos 2\theta$$

$$C_{33} = JZ_1 - \frac{\omega\phi_1}{4} - \frac{3\omega}{4}(2\phi_0 + \phi_1)\cos 2\theta + 2D_3^{(2)}\cos 2\theta$$

Matrix elements of matrix β can be found using the following equation.

$$E(\varepsilon^3) = \varepsilon^2\beta.\vec{\varepsilon}$$

$$\beta_{11} = \frac{\omega}{8}(4\phi_0 + \phi_1)\sin 2\theta - \frac{4D_1^{(2)}\cos\theta\sin\theta}{3}$$

$$\beta_{12} = \beta_{21} = \beta_{23} = \beta_{32} = \frac{3\omega}{8}\phi_1\sin 2\theta$$

$$\beta_{31} = \beta_{13} = 0$$

$$\beta_{22} = \frac{\omega}{4}(2\phi_0 + \phi_1)\sin 2\theta - \frac{4D_2^{(2)}\cos\theta\sin\theta}{3}$$

$$\beta_{33} = \frac{\omega}{8}(4\phi_0 + \phi_1)\sin 2\theta - \frac{4D_3^{(2)}\cos\theta\sin\theta}{3}$$

Matrix elements of matrices F and G can be found using

$$E(\varepsilon^4) = \varepsilon^3 F.\vec{\varepsilon} + \varepsilon^2 G\varepsilon^2$$

$$F_{11} = -\frac{1}{24}\left(JZ_1 - \frac{\omega\phi_1}{4}\right) + \frac{\omega}{8}\left(2\phi_0 + \frac{\phi_1}{4}\right)\cos 2\theta - \frac{D_1^{(2)}\cos 2\theta}{3}$$

$$F_{12} = F_{21} = F_{23} = F_{32} = \frac{1}{6}\left(JZ_1 - \frac{\omega\phi_1}{4}\right) + \frac{\omega}{8}\phi_1\cos 2\theta$$

$$F_{13} = F_{31} = 0$$

$$F_{22} = -\frac{1}{12}\left(JZ_1 - \frac{\omega\phi_1}{4}\right) + \frac{\omega}{8}\left(2\phi_0 + \frac{\phi_1}{2}\right)\cos 2\theta - \frac{D_2^{(2)}\cos 2\theta}{3}$$

$$F_{33} = -\frac{1}{24}\left(JZ_1 - \frac{\omega\phi_1}{4}\right) + \frac{\omega}{8}\left(2\phi_0 + \frac{\phi_1}{4}\right)\cos 2\theta - \frac{D_3^{(2)}\cos 2\theta}{3}$$

$$G_{11} = G_{22} = G_{33} = G_{13} = G_{31} = 0$$

ISSN 1512-1461

$$G_{12}=G_{21}=G_{23}=G_{32}=-\frac{1}{8}\left(JZ_1-\frac{\omega\phi_1}{4}\right)+\frac{3\omega}{32}\phi_1\cos 2\theta$$

After substituting above equations in equation 3,

$$E(\theta)=E_0+\vec{\alpha}.\vec{\varepsilon}+\frac{1}{2}\vec{\varepsilon}.C.\vec{\varepsilon}+\varepsilon^2\beta.\vec{\varepsilon}+\varepsilon^3F.\vec{\varepsilon}+\varepsilon^2G\varepsilon^2 \quad \textbf{(9)}$$

For the minimum energy of the second order-perturbed term [8-10]

$$\vec{\varepsilon}=-C^+.\vec{\alpha} \quad \textbf{(10)}$$

Where C^+ is the pseudo inverse of matrix C, and C^+ can be found using

$$C.C^+=1-\frac{E}{N} \quad \textbf{(11)}$$

Where E is the matrix with all elements given by $E_{mn}=1$.

3. Results and Discussion:

Using a MATLAB program, terms in matrix C^+ were found. After substituting elements of the matrix C^+ in equation 10, $\vec{\varepsilon}$ could be determined. Finally total energy could be found after substituting $\vec{\varepsilon}$ in equation 9. Then equation 9 was divided by ω to write equation in terms of $\frac{E(\theta)}{\omega}$, $\frac{J}{\omega}$, $\frac{D_1^{(2)}}{\omega}$, $\frac{D_2^{(2)}}{\omega}$ and $\frac{D_3^{(2)}}{\omega}$, which are dimensionless parameters. For fcc(001) lattice, Z_0=4, Z_1=4 ,Z_2=0 and Φ_0 = 9.0336 and Φ_1=1.4294 [8, 9, 10]. Figure 1 shows the 3D graph of total energy versus angle and spin exchange interaction for $\frac{D_1^{(2)}}{\omega}=5$, $\frac{D_2^{(2)}}{\omega}=10$ and $\frac{D_3^{(2)}}{\omega}=10$. Peaks along the axis of angle are closely packed in this case compared to the graphs of second and third order perturbed cases [21, 22]. In addition, the shape of this graph is different from the 3D plot of second order and third perturbed cases [21, 22]. One of the energy minimum in this 3D plot can be observed at $\frac{J}{\omega}=10$. Therefore, the graph of total energy versus angle at $\frac{J}{\omega}=10$ is given in figure 2. Energy minimums of this plot can be observed at 0.4084, 2.7332, 3.5500 and 5.8748 radians. Energy maximums can be found at 1.5708, 3.1800 and 4.7124 radians. Major and minor energy maxima can be observed. Energy minima and maxima provide magnetic easy and hard directions, respectively. The angle between adjacent easy and hard directions related to first minima and maxima is 1.1624 radians. Similarly the angle between adjacent easy and hard directions related to second minima and maxima is 1.1624 radians (66.6^0). This implies that the separation between adjacent easy and hard directions remains the same.

ISSN 1512-1461

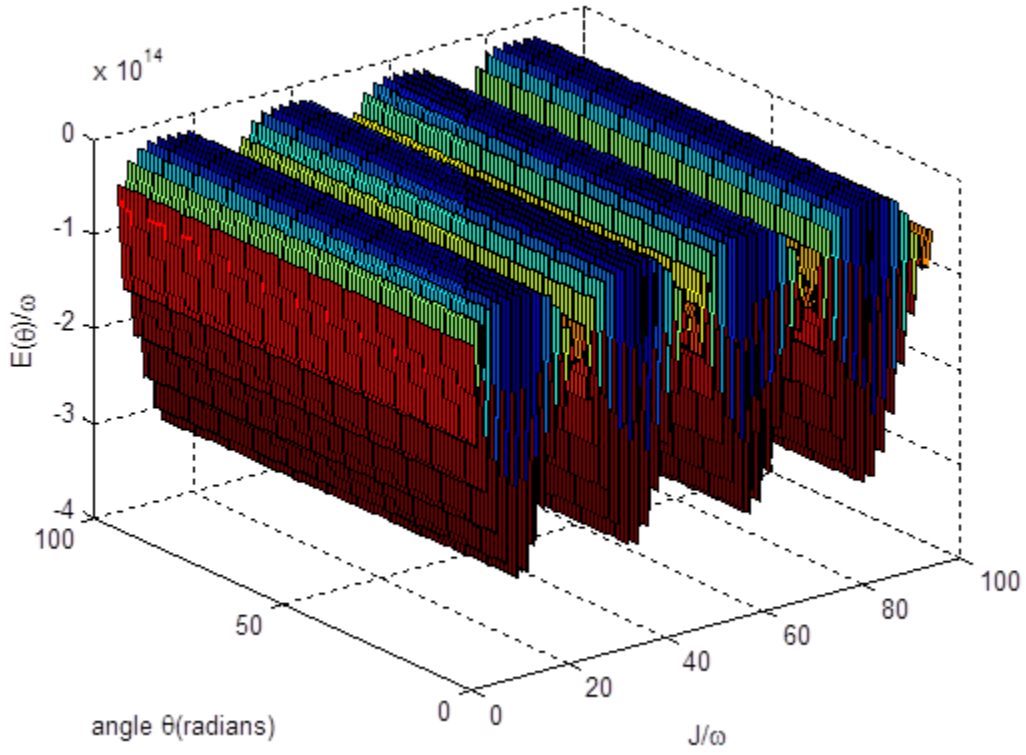

Figure 1: 3D graph of total energy versus angle and spin exchange interaction for $\frac{D_1^{(2)}}{\omega}=5$ $\frac{D_2^{(2)}}{\omega}=10$ and $\frac{D_3^{(2)}}{\omega}=10$.

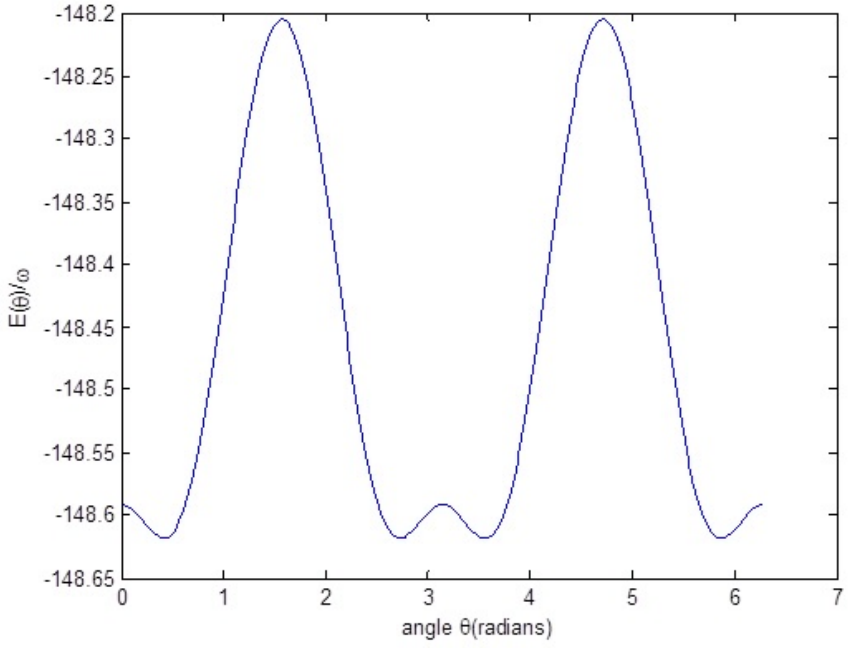

Figure 2: Graph of total energy versus angle at $\frac{J}{\omega}=10$.

ISSN 1512-1461

Figure 3 shows the 3D graph of total energy versus angle and spin exchange interaction for $\frac{D_1^{(2)}}{\omega}=10$, $\frac{D_2^{(2)}}{\omega}=5$ and $\frac{D_3^{(2)}}{\omega}=10$. The total energy in this case (10^{16}) is higher than the total energy (10^{14}) in the 3D plot in figure 1. This implies that when the second order magnetic anisotropy in the middle spin layer is less than those of other two spin layers the total magnetic energy is higher. One of the energy minimum in this graph also can be found at $\frac{J}{\omega}=10$. Figure 4 represents the graph of energy versus angle at $\frac{J}{\omega}=10$. Minor energy maxima observed in figure 2 can not be observed in figure 4. Energy minima can be observed at 0.1885, 3.110 and 6.0947 radians. Energy maxima can be found at 1.5708 and 4.7124 radians. Angle between first adjacent magnetic easy and hard directions is 1.3823 radians (79.2^0). The value of the energy at each energy minimum (or each energy maximum) is the same by implying that the variation is exactly periodic.

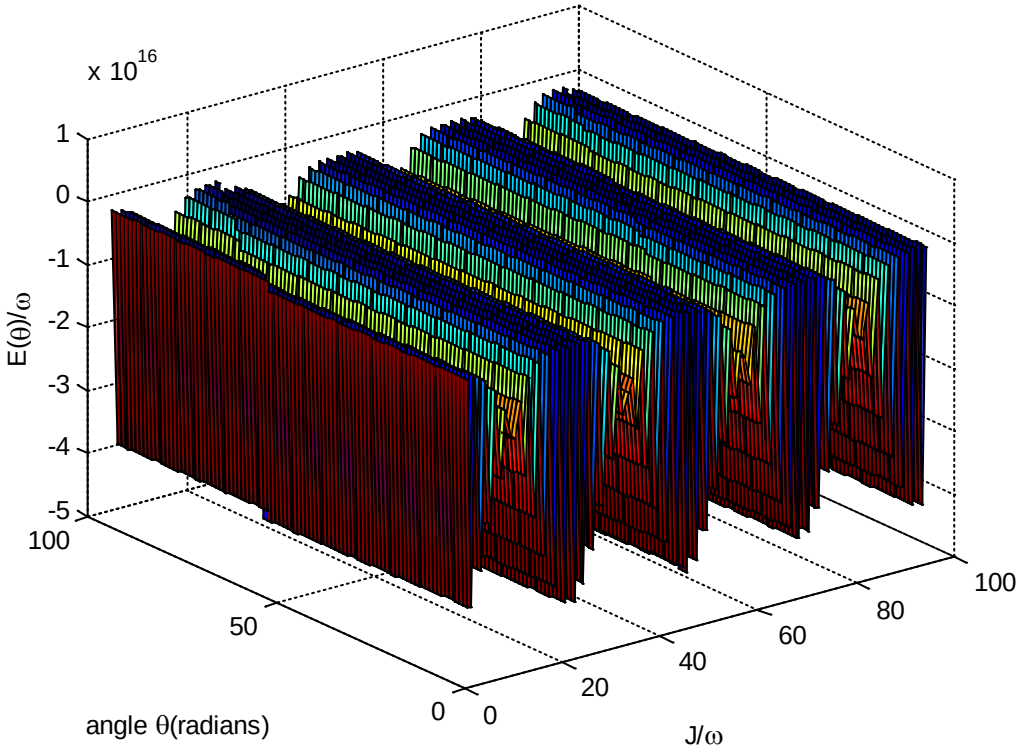

Figure 3: 3D graph of total energy versus angle and spin exchange interaction for $\frac{D_1^{(2)}}{\omega}=10$, $\frac{D_2^{(2)}}{\omega}=5$ and $\frac{D_3^{(2)}}{\omega}=10$.

ISSN 1512-1461

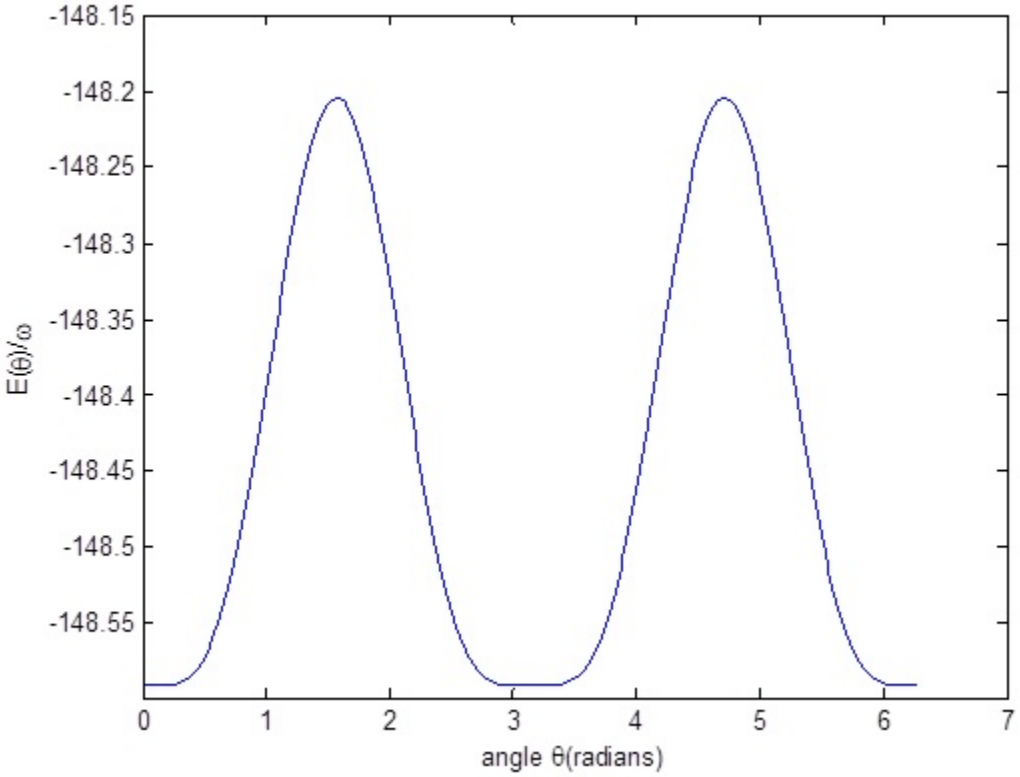

Figure 4: Graph of energy versus angle at $\frac{J}{\omega}=10$.

Figure 5 represents the 3D graph of total energy versus angle and spin exchange interaction for $\frac{D_1^{(2)}}{\omega}=10$, $\frac{D_2^{(2)}}{\omega}=10$ and $\frac{D_3^{(2)}}{\omega}=5$. The energy in this case is in the same order as in the figure 3. These data imply that the energy is less only if the second order magnetic anisotropy constant in the bottom spin layer is less than those of other two spin layers. Thin films with less magnetic energies are said to be soft magnets. According to all the 3D plots given in this manuscript, the peaks along the axis of angle are closely packed. Cross sections of all the 3D plots along the axis of $\frac{J}{\omega}$ are in the same shape. One of the energy minimums in the 3D plot given in the figure 5 can be found at $\frac{J}{\omega}=10$. Figure 6 shows the graph of total magnetic energy versus angle for $\frac{J}{\omega}=10$. Minimums of this graph can be observed at 0.5341, 2.608, 3.676 and 5.718 radians. Energy maximums can be found at 1.571, 3.142 and 4.712 radians. Energy minima and maxima provide magnetic easy and hard directions. In three graphs given in figures 2, 4 and6, angles at maximums (or minimums) are slightly different. The angle between the first adjacent minima and maxima is 1.037 radians (59.41^0). The angle between magnetic easy and hard directions is smallest, when the top spin layer has the lowest second order magnetic anisotropy constant. On the other hand, the angle between magnetic easy and hard directions is highest, when the middle spin layer has the lowest second order magnetic anisotropy constant.

According to experimental studies, the magnetic properties of thin films solely depend on second order magnetic anisotropy constant [30, 31].

ISSN 1512-1461

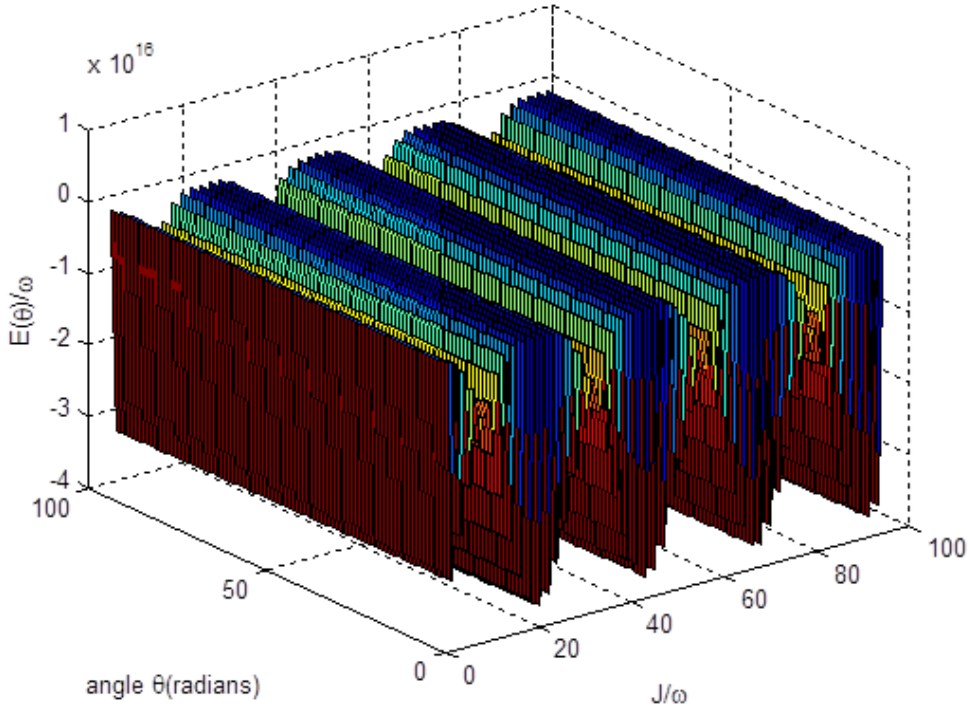

Figure 5: 3D graph of total energy versus angle and spin exchange interaction for $\frac{D_1^{(2)}}{\omega}=10$, $\frac{D_2^{(2)}}{\omega}=10$ and $\frac{D_3^{(2)}}{\omega}=5$.

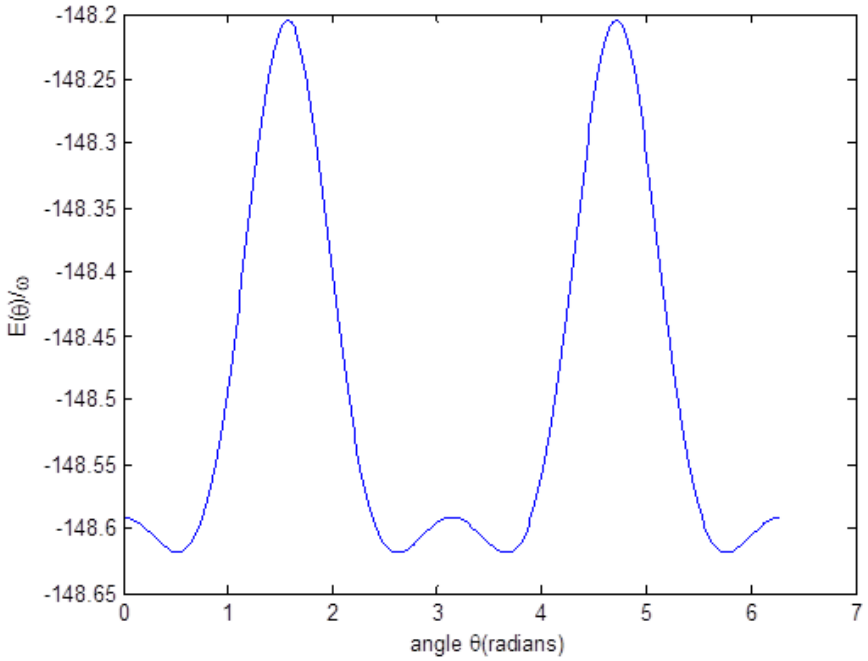

Figure 6: Graph of total magnetic energy versus angle for $\frac{J}{\omega}=10$.

ISSN 1512-1461

4. Conclusion:

For $\frac{D_1^{(2)}}{\omega}=5$, $\frac{D_2^{(2)}}{\omega}=10$, $\frac{D_3^{(2)}}{\omega}=10$ and $\frac{J}{\omega}=10$, energy minimums of the plot can be observed at 0.4084, 2.7332, 3.5500 and 5.8748 radians. Energy maximums can be found at 1.5708, 3.1800 and 4.7124 radians. The angle between adjacent easy and hard directions related to first minima and maxima is 1.1624 radians. Similarly the angle between adjacent easy and hard directions related to second minima and maxima is 1.1624 radians (66.6^0) in this case. For $\frac{D_1^{(2)}}{\omega}=10$, $\frac{D_2^{(2)}}{\omega}=10$, $\frac{D_3^{(2)}}{\omega}=5$ and $\frac{J}{\omega}=10$, minimums of the graph can be observed at 0.5341, 2.608, 3.676 and 5.718 radians. Energy maximums can be found at 1.571, 3.142 and 4.712 radians. The angle between the first adjacent minima and maxima is 1.037 radians (59.41^0) in this case. The angle between magnetic easy and hard directions is least, when the top spin layer has the lowest second order magnetic anisotropy constant. The angle between magnetic easy and hard directions is highest, when the middle spin layer has the lowest second order magnetic anisotropy constant.

References:

1. L. Dreher, M. Weiler, M. Pernpeintner, H. Huebi, R. Gross, M.S. Brandt and S.T.B. Goennenwein (2012). Surface acoustic wave driven ferromagnetic resonance in nickel thin films: Theory and experiment. *Physical Review B* **86**: 134415.
2. S. Azzawi, A.T. Hindmarch and D. Atkinson (2017). Magnetic damping phenomena in ferromagnetic thin films and multilayers. *Journal of Physics D: Applied Physics* **50**: 473001.
3. Radomska Anna and Balcerzak Tadeusz (2003). Theoretical studies of model thin EuTe films with surface elastic stresses. *Central European Journal of Physics* **1(1)**: 100-117.
4. C. Cates James and Alexander Jr Chester. (1994). Theoretical study of magnetostriction in FeTaN thin films. *Journal of Applied Physics* **75**: 6754-6756.
5. A. Ernst, M. Lueders, W.M. Temmerman, Z. Szotek and G. Van der Laan (2000). Theoretical study of magnetic layers of nickel on copper; dead or live?. *Journal of Physics: Condensed matter* **12(26)**: 5599-5606.
6. Kovachev St and J.M. Wesselinowa (2009). Theoretical study of multiferroic thin films based on a microscopic model. *Journal of Physics: Condensed matter* **21(22)**: 225007.
7. Tsai Shan-Ho, D.P. Landau and C. Schulthess Thomas (2003). Effect of interfacial coupling on the magnetic ordering in ferro-antiferromagntic bilayers. *Journal of Applied Physics* **93(10)**: 8612-8614.
8. A. Hucht and K.D. Usadel. (1997). Reorientation transition of ultrathin ferromagnetic films. *Physical Review B* **55**: 12309.
9. A. Hucht and K.D. Usadel (1999). Theory of the spin reorientation transition of ultra-thin ferromagnetic films. *Journal of Magnetism and Magnetic materials* **203(1)**: 88-90.
10. K.D. Usadel and A. Hucht (2002). Anisotropy of ultrathin ferromagnetic films and the spin reorientation transition. *Physical Review B* **66**: 024419.
11. U. Nowak (1995). Magnetisation reversal and domain structure in thin magnetic films: Theory and computer simulation. *IEEE transaction on magnetics* **31(6-2)**: 4169-4171.
12. M. Dantziger, B. Glinsmann, S. Scheffler, B. Zimmermann and P.J. Jensen (2002). In-plane dipole coupling anisotropy of a square ferromagnetic Heisenberg monolayer. *Physical Review B* **66**: 094416.
13. H. Hegde, P. Samarasekara and F.J. Cadieu (1994). Nonepitaxial sputter synthesis of aligned strontium hexaferrites, SrO.6(Fe_2O_3), films. *Journal of Applied Physics* **75(10):** 6640-6642.
14. P. Samarasekara (2003). A Pulsed RF Sputtering Method for Obtaining Higher Deposition

ISSN 1512-1461

Rates. *Chinese Journal of Physics* **41(1):** 70-74.
15. P. Samarasekara and F.J. Cadieu. (2001). Magnetic and Structural Properties of RF Sputtered Polycrystalline Lithium Mixed Ferrimagnetic Films. *Chinese Journal of Physics* **39(6):** 635-640.
16. P. Samarasekara (2010). Determination of Energy of thick spinel ferrite films using Heisenberg Hamiltonian with second order perturbation" *Georgian electronic scientific journals: Physics* **1(3):** 46-52.
17. P. Samarasekara, M.K. Abeyratne and S. Dehipawalage (2009). Heisenberg Hamiltonian with Second Order Perturbation for Spinel Ferrite Thin Films. *Electronic Journal of Theoretical Physics* **6(20):** 345-356.
18. P. Samarasekara and N.H.P.M. Gunawardhane (2011). Explanation of easy axis orientation of ferromagnetic films using Heisenberg Hamiltonian. *Georgian electronic scientific journals: Physics* **2(6)**: 62-69.
19. P. Samarasekara and S.N.P. De Silva (2007). Heisenberg Hamiltonian solution of thick ferromagnetic films with second order perturbation. *Chinese Journal of Physics* **45(2-I):** 142-150
20. P. Samarasekara (2008). Influence of third order perturbation on Heisenberg Hamiltonian of thick ferromagnetic films. *Electronic Journal of Theoretical Physics* **5(17):** 227-236.
21. P. Samarasekara (2006). Second order perturbation of Heisenberg Hamiltonian for non-oriented ultra-thin ferromagnetic films. *Electronic Journal of Theoretical Physics* **3(11):** 71-83.
22. P. Samarasekara and William A. Mendoza (2010). Effect of third order perturbation on Heisenberg Hamiltonian for non-oriented ultra-thin ferromagnetic films. *Electronic Journal of Theoretical Physics* **7(24)**: 197-210.
23. P. Samarasekara (2007). Classical Heisenberg Hamiltonian Solution of Oriented Spinel Ferrimagnetic Thin Films. *Electronic Journal of Theoretical Physics* **4(15):** 187-200.
24. P. Samarasekara (2011). Investigation of Third Order Perturbed Heisenberg Hamiltonian of Thick Spinel Ferrite Films. *Inventi Rapid: Algorithm Journal* **2(1)**: 1-3.
25. F. Virot, L. Favre, R. Hayn and M.D. Kuzmin (2012). Theory of magnetic domains in uniaxial thin films. *Journal of Physics D: Applied Physics* **45**: 405003.
26. Y. Laosiritaworn, R. Yimnirun and J. Poulter (2006). The effect of uniaxial stress to spin reorientation transition in magnetic thin films: Monte Carlo investigation. *Current Applied Physics* **6(3)**: 469-473.
27. C. Santamaria and H.T. Diep (2000). Dipolar interactions in magnetic thin films: perpendicular to in-plane ordering transition. *Journal of magnetism and magnetic materials* **212(1-2)**: 23-38.
28. V. T. Ngo and H.T. Diep (2007). Effects of frustrated surface in Heisenberg thin films. *Physical Review B* **75**: 035412.
29. D. Spenato, A. Fessant, J. Gieraltowski, J. Loaec and H. Le Gall (1993). Theoretical and experimental approach of spin dynamics in in-plane anisotropic amorphous ferromagnetic thin films. *Journal of Physics D: Applied Physics* **26**: 1736.
30. H. Stillrich, C. Menk, R. Fromter and H.P. Oepen (2009). Magnetic anisotropy and the cone state in Co/Pt multilayer films. *Journal of Applied Physics* **105**: 07C308.
31. H.K. Gweon and S.H. Lim (2020). Evolution of strong second order magnetic anisotropy in Pt/Co/MgO trilayers by post annealing. *Applied Physics Letters* **117**: 082403.

Article received 2022-06-06